

Origin of the large polarization in multiferroic YMnO₃ thin films revealed by soft and hard x-ray diffraction

H. Wadati,^{1,*} J. Okamoto,² M. Garganourakis,³ V. Scagnoli,³ U. Staub,³ Y. Yamasaki,²
H. Nakao,² Y. Murakami,² M. Mochizuki,¹ M. Nakamura,⁴ M. Kawasaki,^{1,4} and Y. Tokura,^{1,4}

¹*Department of Applied Physics and Quantum-Phase Electronics Center (QPEC),
University of Tokyo, Hongo, Tokyo 113-8656, Japan*

²*Condensed Matter Research Center and Photon Factory, Institute of Materials Structure Science,
High Energy Accelerator Research Organization, Tsukuba 305-0801, Japan*

³*Swiss Light Source, Paul Scherrer Institut, 5232 Villigen PSI, Switzerland*

⁴*Cross-Correlated Materials Research Group (CMRG),
RIKEN Advanced Science Institute, Wako 351-0198, Japan*

(Dated: September 13, 2011)

We investigated the magnetic structure of an orthorhombic YMnO₃ thin film by resonant soft x-ray and hard x-ray diffraction. We observed a temperature-dependent incommensurate magnetic reflection below 45 K and a commensurate lattice-distortion reflection below 35 K. These results demonstrate that the ground state is composed of coexisting E-type and cycloidal states. Their different ordering temperatures clarify the origin of the large polarization to be caused by the E-type antiferromagnetic states in the orthorhombic YMnO₃ thin film.

Recently, there has been a lot of interest in multiferroic materials, which display both ferroelectric and magnetic orders with giant magnetoelectric coupling [1–3]. It is of particular importance to control magnetization (electric polarization) by electric (magnetic) field for novel device applications. Orthorhombic (*o*-) *RMnO₃* (*R*: rare-earth) with perovskite structure are prototype multiferroic materials. For example, in TbMnO₃, ferroelectricity occurs below 28 K, concomitant with the onset of cycloidal spin ordering [4–6]. The ferroelectricity in the cycloidal states is realized by the shifts of the oxygen ions through the inverse Dzyaloshinskii-Moriya interaction [7, 8]. This is in contrast to E-type antiferromagnetic structures ($\uparrow\downarrow\downarrow$ type), where ferroelectricity is caused by symmetric exchange striction [9]. E-type magnetic structures occur in *o*-*RMnO₃* with smaller *R* ions. It is predicted that the E-type structure leads to a larger polarization, which has been experimentally confirmed in the *o*-*RMnO₃* systems [10, 11].

The fabrication of the *o*-*RMnO₃* thin films has been especially important for device application of the multiferroic materials. Moreover, bulk *o*-*RMnO₃* samples with smaller *R* ions (*R* = Y, Ho - Lu) can only be synthesized under high oxygen pressure [11], which strongly limits studies on the most interesting materials due to the absence of significantly large high-quality single crystals. Recently, Nakamura *et al.* reported the fabrication of *o*-YMnO₃ thin films onto the YAlO₃ (010) substrate [12]. Their thin film showed a ferroelectric transition at 40 K with a large saturation polarization of 0.8 $\mu\text{C}/\text{cm}^2$. The ferroelectric polarization could be controlled by magnetic fields, demonstrating magnetoelectric behaviors.

Therefore it is interesting and important to clarify the exact magnetic structure of YMnO₃ thin films. In this study we use the technique of resonant soft x-ray diffraction at Mn $2p \rightarrow 3d$ edges to obtain the informa-

tion of magnetic ordering in YMnO₃ thin films. Resonant soft x-ray diffraction has recently been used to study the magnetic ordering in multiferroic TbMnO₃ and Eu_{3/4}Y_{1/4}MnO₃ [13–15] using single crystals for the larger *R*-ion orthorhombic *RMnO₃* series. This technique is especially suitable for studying magnetism in thin films (as demonstrated on *RNiO₃* [16]) because even small sample volume of thin films can be used due to the large resonant enhancement of magnetic scattering at the transition-metal $2p \rightarrow 3d$ edges. We detect (0 q_b 0) ($q_b \sim 0.5$) magnetic peak, and observed temperature-dependent incommensurabilities. From hard x-ray diffraction we found a commensurate superlattice reflection (0 1 0) that reflects the lattice distortion caused by the E-type magnetic structure. These results reveal that the ground state of the YMnO₃ can be described by the coexistence of E-type and cycloidal states, while the E-type state is a dominant source for the large electric polarization of 0.8 $\mu\text{C}/\text{cm}^2$ by the symmetric exchange striction.

The thin film (40 nm) of YMnO₃ was grown on a YAlO₃ (010) substrate by pulsed-laser deposition. The details of the sample fabrication were described elsewhere [12]. Resonant soft x-ray diffraction experiments were performed on the RESOXS endstation [17] at the surfaces/interfaces microscopy (SIM) beamline of the Swiss Light Source of the Paul Scherrer Institut, Switzerland. For the azimuthal scans (rotation around the Bragg scattering wave vector), the sample transfer line was used to rotate the sample holder. With pins attached in a threefold symmetry on the sample holder, an accuracy of approximately 5 deg was obtained. A continuous helium-flow cryostat allows measurements between 10 and 300 K. Hard x-ray diffraction experiments were performed on beamlines 3A and 4C at the Photon Factory, KEK, Japan. The photon energy of the incident x-ray was 12

keV.

Figure 1 shows the temperature dependence of the $(0\ q_b\ 0)$ ($q_b \sim 0.5$) peak with π (a) and σ (b) incident x-ray polarizations. The experimental geometry is shown in Fig. 1 (c), together with the definition of the azimuthal angle φ . Here the diffraction data were taken with $\varphi = 0^\circ$ at $h\nu = 643.1$ eV (Mn $2p_{3/2} \rightarrow 3d$ absorption edge). We measured in both cooling and heating cycles, and observed no hysteresis behavior. This peak, which is indicated by vertical bars, appears at 45 K, which coincides with the antiferromagnetic transition temperature T_N determined from magnetization measurements [12]. Weaker peaks are observed on both sides of the reflection. These are antiferromagnetic Kiessig fringes, and describe the limited thickness of the magnetic contrast of the film. There is almost no difference between π (a) and σ (b) polarizations. The intensity of the peaks increases monotonically with cooling. The peak position deviates from the commensurate $q_b = 1/2$ position for all temperatures. The peak position shifts to higher angle for decreasing temperatures; the temperature variation of the corresponding wave vector and intensity is summarized in Fig. 2. The intensity increases monotonically and smoothly with decreasing temperatures from $T_N = 45$ K. The peak position, e.g. $q_b = 0.457$ at 44 K and 0.491 at 11 K, is temperature-dependent and always incommensurate ($\neq 1/2$) in the temperature range of 11 - 44 K. In TbMnO_3 the peak position is also incommensurate, but lock to the value of $q_b = 0.285$ at the ferroelectric transition temperature $T_C = 28$ K [13, 14]. Such a behavior is not observed in this YMnO_3 film; there is no locking of the peak position at $T_C = 40$ K, which was determined from electric polarization measurements [12].

Figure 3 shows the intensity of the $(0\ q_b\ 0)$ ($q_b \sim 0.5$) peak as a function of photon energies at the Mn $2p \rightarrow 3d$ absorption edge at 44 K (a) and 11 K (b). There is no polarization dependence at this scattering geometry of $\varphi = 0^\circ$ at both temperatures. In addition, the spectral shape is identical at these two temperatures and very similar to the one observed for TbMnO_3 and $\text{Eu}_{3/4}\text{Y}_{1/4}\text{MnO}_3$ [13–15]. This shows that the line shape of the spectrum does not depend on the values of q_b but is rather common in multiferroic $o\text{-RMnO}_3$.

To gain more information on the spin structure, it is important to study the magnetic reflection with linear polarized incident radiation for different azimuthal angles. The φ (azimuthal angle) dependence of the intensity of the magnetic $(0\ q_b\ 0)$ reflection is shown in Fig. 4. For $\varphi = 0^\circ$, the intensities are identical for π and σ polarizations within experimental uncertainty. When φ increases from 0° to 90° , the intensity increases with incident π polarization and decreases with incident σ polarization. The azimuthal-angle dependence allows us to gain information on the directions of the Mn spins. In the electric-dipole transition, the magnetic contribution

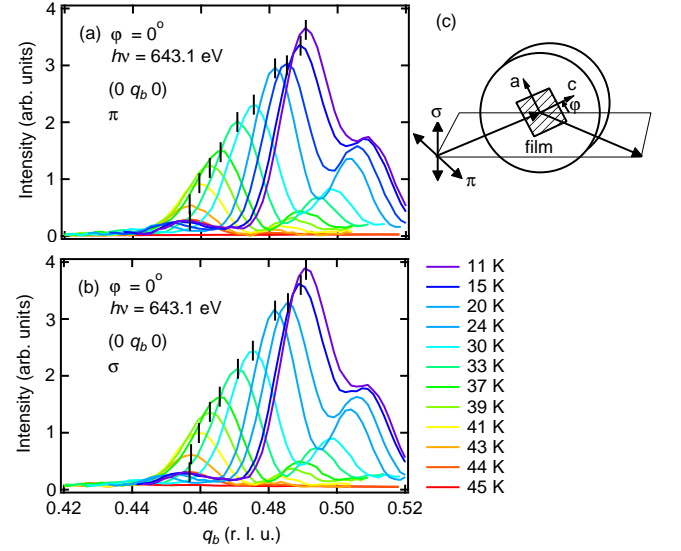


FIG. 1: (Color online): Temperature dependence of the $(0\ q_b\ 0)$ ($q_b \sim 0.5$) peak in π (a) and σ (b) incident x-ray polarizations. Panel (c) shows the experimental geometry with the definition of the azimuthal angle φ . In panels (a) and (b), the data were taken with $\varphi = 0^\circ$ at $h\nu = 643.1$ eV (Mn $2p_{3/2} \rightarrow 3d$ absorption edge).

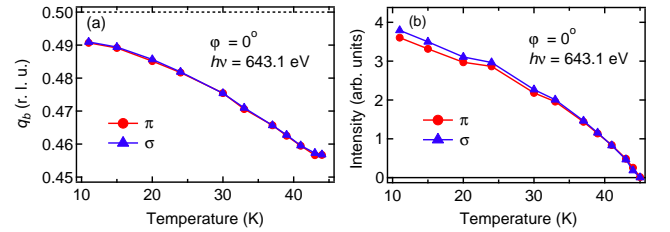


FIG. 2: (Color online): Temperature dependence of the $(0\ q_b\ 0)$ ($q_b \sim 0.5$) peak position (a) and intensity (b). The experimental geometry and the photon energy are the same as Fig. 1. In panel (a), the commensurate position of $q_b = 1/2$ is shown as a dotted line.

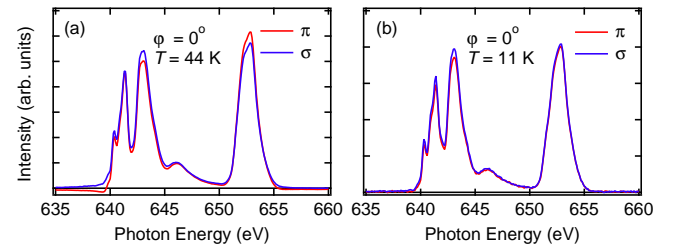


FIG. 3: (Color online): Intensity of the $(0\ q_b\ 0)$ ($q_b \sim 0.5$) peak as a function of photon energies at the Mn $2p \rightarrow 3d$ absorption edge at 44 K (a) and 11 K (b).

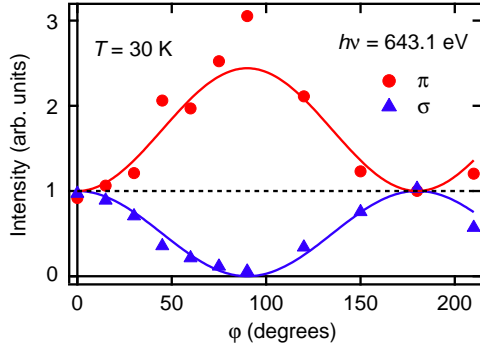


FIG. 4: (Color online): Azimuthal angle dependence of the $(0 q_b 0)$ ($q_b \sim 0.5$) intensity. The solid lines are from the model with spins parallel to the c axis.

to the structure factor is given as

$$f_{mag}^{res} \propto (\hat{\epsilon}' \times \hat{\epsilon}) \cdot \hat{z},$$

where $\hat{\epsilon}$ and $\hat{\epsilon}'$ are unit vectors of the incident and scattered polarization, respectively, and \hat{z} is a unit vector in the direction of the magnetic moment of the ion [18, 19]. We use the notations in Fig. 1 in Ref. [19] which lead to the following expression,

$$(\hat{\epsilon}' \times \hat{\epsilon}) \cdot \hat{z} = \begin{pmatrix} 0 & z_1 \cos \theta_B + z_3 \sin \theta_B \\ z_3 \sin \theta_B - z_1 \cos \theta_B & -z_2 \sin 2\theta_B \end{pmatrix}$$

Here θ_B is the Bragg angle for the $(0 q_b 0)$ reflection. When the magnetic Fourier components contribute only along the c axis, $z_1 = \cos \varphi$, $z_2 = \sin \varphi$, and $z_3 = 0$. Then the intensity for π and σ incident polarizations are given with $\theta_B \sim 51.5^\circ$ at 30 K.

$$\begin{aligned} I(\pi) &= |I(\pi \rightarrow \sigma')|^2 + |I(\pi \rightarrow \pi')|^2 \\ &= |\cos \varphi \cos \theta|^2 + |\sin \varphi \sin 2\theta|^2 \\ &\sim 0.95 - 0.56 \cos^2 \varphi \\ I(\sigma) &= |I(\sigma \rightarrow \pi')|^2 \\ &= |\cos \varphi \cos \theta|^2 \\ &\sim 0.39 \cos^2 \varphi \end{aligned}$$

The values of these equations are shown as solid lines in Fig. 4, and are in good agreement with our experimental observations. This reflects an ab cycloid with a spin canting along the c -axis as shown in Fig. 5, and indicates that the experiment is only sensitive to its magnetic sinusoidal c axis component.

In order to investigate the lattice distortions associated with magnetic order and electric polarization, we additionally performed hard x-ray diffraction measurements of the YMnO₃ thin film. The commensurate $(0 1 0)$ reflection appears below 35 K as shown in Fig. 6. This reflection is a structurally forbidden in the chemical high-temperature structure (Pbnm) and caused by

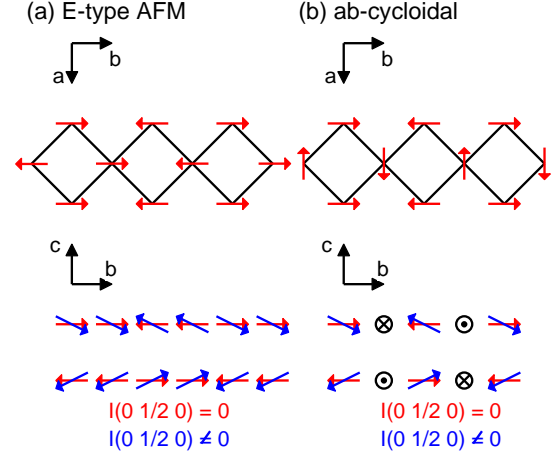


FIG. 5: (Color online): Spin structures in the E-type (a) and the ab -cycloidal (b) states. Spin canting along the c axis makes the magnetic $(0 q_b 0)$ peak have some intensity.

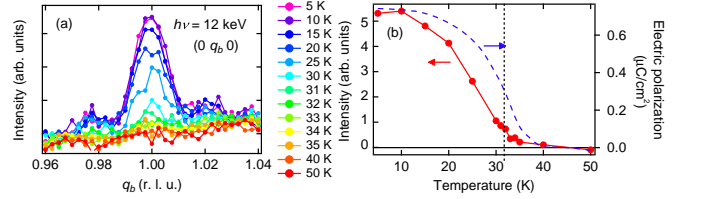


FIG. 6: (Color online): Temperature dependence of the $(0 1 0)$ peak taken at $h\nu = 12$ keV. In panel (b), peak intensities are plotted as a function of temperature together with the electric polarization (broken lines) taken from Ref. [12]. The temperature of 35 K is also indicated as the onset of the $(0 1 0)$ peak and the step onset of the spontaneous electric polarization.

the lattice distortion accompanying ferroelectricity. Interestingly, no incommensurability of this reflection is observed by hard x-ray diffraction, in clear contrast to the observed magnetic reflection. Moreover, this reflection does appear below 35 K, at lower temperatures than the onset of the magnetic reflection, in accord with the step onset of the spontaneous electric polarization [12], as can be seen from the temperature-dependent integrated intensity shown in Fig. 6 (b).

We can obtain a full picture of the magnetic states of the epitaxial YMnO₃ thin film by combining the above results with the macroscopic measurements of magnetization and electric polarization [12]. From the macroscopic measurements, three transitions were observed: antiferromagnetic transition at $T_N = 45$ K, ferroelectric transition at $T_C = 40$ K, and an increase of electric polarization at 35 K. The incommensurate magnetic peak was observed at all temperature below 45 K. It reflects spin moments solely along the c axis as indicated by its x-

ray polarization and azimuthal dependence. This supports the scenario that in the temperature range of 40 - 45 K a sinusoidal state with a spin canting along the c axis is realized. Note that the in-plane magnetic moment components cancel for this magnetic wave vector in the structure factor. This state is also consistent with the absence of observed electric polarization in this temperature regime (see Fig. 6 (b)). By cooling through 40 K, the sinusoidal magnetic phase transforms into a cycloidal magnetic structure with significant magnetic moment contributions along the c axis. Below 35 K, we can observe both the incommensurate magnetic reflection and the commensurate lattice-distortion reflection. This state can be therefore explained by the coexistence of the cycloidal and the E-type states as theoretically predicted in Ref. [20]. In this coexistence region, magnetic reflection is incommensurate as shown in Ref. [20] and lattice peaks are commensurate because the E-type phase has a much larger lattice distortion than the cycloidal phase. The existence of the E-type phase causes the large electric polarization of $0.8 \mu\text{C}/\text{cm}^2$ due to the symmetric exchange striction [12]. In other words, the weak polarization emerging at 40 K from the cycloidal magnetic structure causes also weak lattice distortion, which is too weak to be observed in our experiment. On the other hand, the large induced electric polarization below 35 K caused by the E-type structure induces a significant lattice distortion, as observed by the x-ray diffraction experiments on a YMnO_3 single crystal [21]. However, spin canting in its magnetic structure is so small that no additional magnetic contribution is observed in our experiment. It is difficult to distinguish between the occurrence of ab - and bc -cycloids based on our experimental data. However, electric polarization is parallel to the a axis [12], which clearly indicates the ab -cycloid. The ab -cycloids can easily adopt a spin canting along the c axis, whereas bc -cycloids would get anisotropically distorted.

In summary, we investigated the magnetic structures of the YMnO_3 thin film by resonant magnetic soft x-ray and hard x-ray diffraction. We observed temperature-dependent incommensurate magnetic peaks below 45 K and commensurate lattice-distortion peaks below 35 K, indicating that E-type and cycloidal states coexist below 35 K. This shows that the occurrence of the large electric polarization below 35 K is directly related to E-type magnetic ordering component in the epitaxial YMnO_3 films.

Informative discussions with S. Ishiwata are greatly acknowledged. The authors thank the experimental support of the X11MA beamline staff. Financial support of the Swiss National Science Foundation and its NCCR MaNEP is gratefully acknowledged. This work is also supported by the Japan Society for the Promotion of Science (JSPS) through its Funding Program for World-Leading Innovative R&D on Science and Technology (FIRST Program). Hard x-ray diffraction measurements

were performed under the approval of the Photon Factory Program Advisory Committee (Proposals Nos. 2009S2-008 and 2010G678) at the Institute of Material Structure Science, KEK.

* Electronic address: wadati@ap.t.u-tokyo.ac.jp;
URL: <http://www.geocities.jp/qxbqd097/index2.htm>

- [1] Y. Tokura, Science **312**, 1481 (2006).
- [2] S.-W. Cheong and M. Mostovoy, Nature Mater. **6**, 13 (2007).
- [3] Y. Tokura and S. Seki, Adv. Mater. **22**, 1554 (2010).
- [4] T. Kimura, T. Goto, H. Shintani, K. Ishizaka, T. Arima, and Y. Tokura, Nature **426**, 55 (2003).
- [5] T. Kimura, G. Lawes, T. Goto, Y. Tokura, and A. P. Ramirez, Phys. Rev. B **71**, 224425 (2005).
- [6] M. Kenzelmann, A. B. Harris, S. Jonas, C. Broholm, J. Schefer, S. B. Kim, C. L. Zhang, S.-W. Cheong, O. P. Vajk, and J. Lynn, Phys. Rev. Lett. **95**, 087206 (2005).
- [7] H. Katsura, N. Nagaosa, and A. V. Balatsky, Phys. Rev. Lett. **95**, 057205 (2005).
- [8] M. Mostovoy, Phys. Rev. Lett. **96**, 067601 (2006).
- [9] I. A. Sergienko and E. Dagotto, Phys. Rev. B **73**, 094434 (2006).
- [10] V. Y. Pomjakushin, M. Kenzelmann, A. Donni, A. B. Harris, T. Nakajima, S. Mitsuda, M. Tachibana, L. Keller, J. Mesot, H. Kitazawa, and E. Takayama-Muromachi, New J. Phys. **11**, 043019 (2009).
- [11] S. Ishiwata, Y. Kaneko, Y. Tokunaga, Y. Taguchi, T. Arima, and Y. Tokura, Phys. Rev. B **81**, 100411(R) (2010).
- [12] M. Nakamura, Y. Tokunaga, M. Kawasaki, and Y. Tokura, Appl. Phys. Lett. **98**, 082902 (2011).
- [13] T. R. Forrest, S. R. Bland, S. B. Wilkins, H. C. Walker, T. A. W. Beale, P. D. Hatton, D. Prabhakaran, A. T. Boothroyd, D. Mannix, F. Yakhov, and D. F. McMorrow, J. Phys. Condens. Matter **20**, 422205 (2008).
- [14] S. B. Wilkins, T. R. Forrest, T. A. W. Beale, S. R. Bland, H. C. Walker, D. Mannix, F. Yakhov, D. Prabhakaran, A. T. Boothroyd, J. P. Hill, P. D. Hatton, and D. F. McMorrow, Phys. Rev. Lett. **103**, 207602 (2009).
- [15] H. Jang, J.-S. Lee, K.-T. Ko, W.-S. Noh, T. Y. Koo, J.-Y. Kim, K.-B. Lee, J.-H. Park, C. L. Zhang, S. B. Kim, and S.-W. Cheong, Phys. Rev. Lett. **106**, 047203 (2011).
- [16] V. Scagnoli, U. Staub, A. M. Mulders, M. Janousch, G. I. Meijer, G. Hammerl, J. M. Tonnerre, and N. Stojic, Phys. Rev. B **73**, 100409(R) (2006).
- [17] U. Staub, V. Scagnoli, Y. Bodenthin, M. Garcia-Fernandez, R. Wetter, A. M. Mulders, H. Grimmer, and M. Horisberger, J. Synchrotron Radiat. **15**, 469 (2008).
- [18] J. P. Hannon, G. T. Trammell, M. Blume, and D. Gibbs, Phys. Rev. Lett. **61**, 1245 (1988).
- [19] J. P. Hill and D. F. McMorrow, Acta Crystallogr. Sect. A **52**, 236 (1996).
- [20] M. Mochizuki, N. Furukawa, and N. Nagaosa, Phys. Rev. Lett. **105**, 037205 (2010).
- [21] D. Okuyama, S. Ishiwata, Y. Takahashi, K. Yamauchi, S. Picozzi, K. Sugimoto, H. Sakai, M. Takata, R. Shimano, Y. Taguchi, T. Arima, and Y. Tokura, Phys. Rev. B **84**, 054440 (2011).